SREBP2 delivery to striatal astrocytes normalizes cholesterol biosynthesis and ameliorates pathological features in Huntington's Disease

Giulia Birolini[1,2], Gianluca Verlengia[3,4], Francesca Talpo[5], Claudia Maniezzi[5], Lorena Zentilin[6], Mauro Giacca[6,7], Paola Conforti[1,2], Chiara Cordiglieri[2], Claudio Caccia[8], Valerio Leoni[9], Franco Taroni[8], Gerardo Biella[5], Michele Simonato[3,4], Elena Cattaneo[1,2], Marta Valenza[1,2]

[1]Department of Biosciences, University of Milan, via G. Celoria 26, 20133, Milan, Italy. [2]Istituto Nazionale di Genetica Molecolare "Romeo ed Enrica Invernizzi" via F. Sforza 35, 20122, Milan, Italy. [3]Division of Neuroscience, IRCCS San Raffaele Hospital, via Olgettina 58, 20132, Milan, Italy. [4]Department of BioMedical Sciences, Section of Pharmacology, University of Ferrara, via Fossato di Mortara 17-19, 44121, Ferrara, Italy. [5]Department of Biology and Biotechnologies, University of Pavia, Via A. Ferrata, 9, 27100, Pavia, Italy. [6]International Centre for Genetic Engineering and Biotechnology, ICGEB, Padriciano 99, 34149 Trieste, Italy. [7]School of Cardiovascular Medicine & Sciences, King's College London, 125 Coldharbour Lane London SE5 9NU, UK. [8]Unit of Medical Genetics and Neurogenetics. Fondazione I.R.C.C.S. Istituto Neurologico Carlo Besta, Via Celoria 11, 20131 Milan, Italy. [9]School of Medicine and Surgery, University of Milano-Bicocca, Via Cadore 48, 20900, Monza and Laboratory of Clinical Pathology, Hospital of Desio, ASST-Monza.

Email of presenting author: giulia.birolini@unimi.it

Abstract

Cholesterol is a multifaceted molecule essential for brain function (Dietschy & Turley, 1968). In the adult brain, cholesterol is produced locally by astrocytes and transferred to neurons through apoE-containing lipoproteins (Jurevics & Morell 1995). Disruption of brain cholesterol pathways has been linked to several neurological disorders, including Huntington's disease (HD), a genetic, neurodegenerative disorder caused by a CAG expansion in the gene encoding the Huntingtin protein (Valenza & Cattaneo 2011). Brain cholesterol biosynthesis and content are reduced in several HD models (Valenza et al., 2005; 2007; 2010; Shankaran et al., 2017). The underlying molecular mechanism relies on reduced nuclear translocation of SREBP2, the transcription factor that controls the transcription of several genes involved in cholesterol biosynthesis (Valenza et al., 2015; Di Pardo et al., 2020). We have recently shown that cholesterol supplementation to the HD brain ameliorates synaptic and behavioral defects in two mouse models of HD (Valenza et al., 2015; Birolini et al., 2020; Birolini et al. 2021).

Here, we used recombinant adeno-associated virus 2/5 to deliver exogenous SREBP2 specifically in astrocytes in order to enhance the endogenous cholesterol biosynthesis in the striatum of HD mice.

We found that exogenous SREBP2 stimulates the transcription of some of the cholesterol biosynthesis genes resulting in fully restoration of synaptic transmission, reversal of Drd2 transcript levels, clearance of mutant Huntingtin (muHTT) aggregates and rescue of behavioral deficits.

These results demonstrate that stimulating cholesterol biosynthesis in HD brain has a positive effect on behavioral decline and HD-related phenotypes. Furthermore, we have demonstrated that glial SREBP2 participates in HD pathogenesis in vivo, highlighting the translational potential of cholesterol-based strategies for this disease.

Funded by Telethon Foundation (GGP17102), NeurostemcellRepair (FP7, GA no. 602278, 2013-2017), Linea 2-2017 (University of Milan).

Cholesterol biosynthesis is reduced in the HD brain

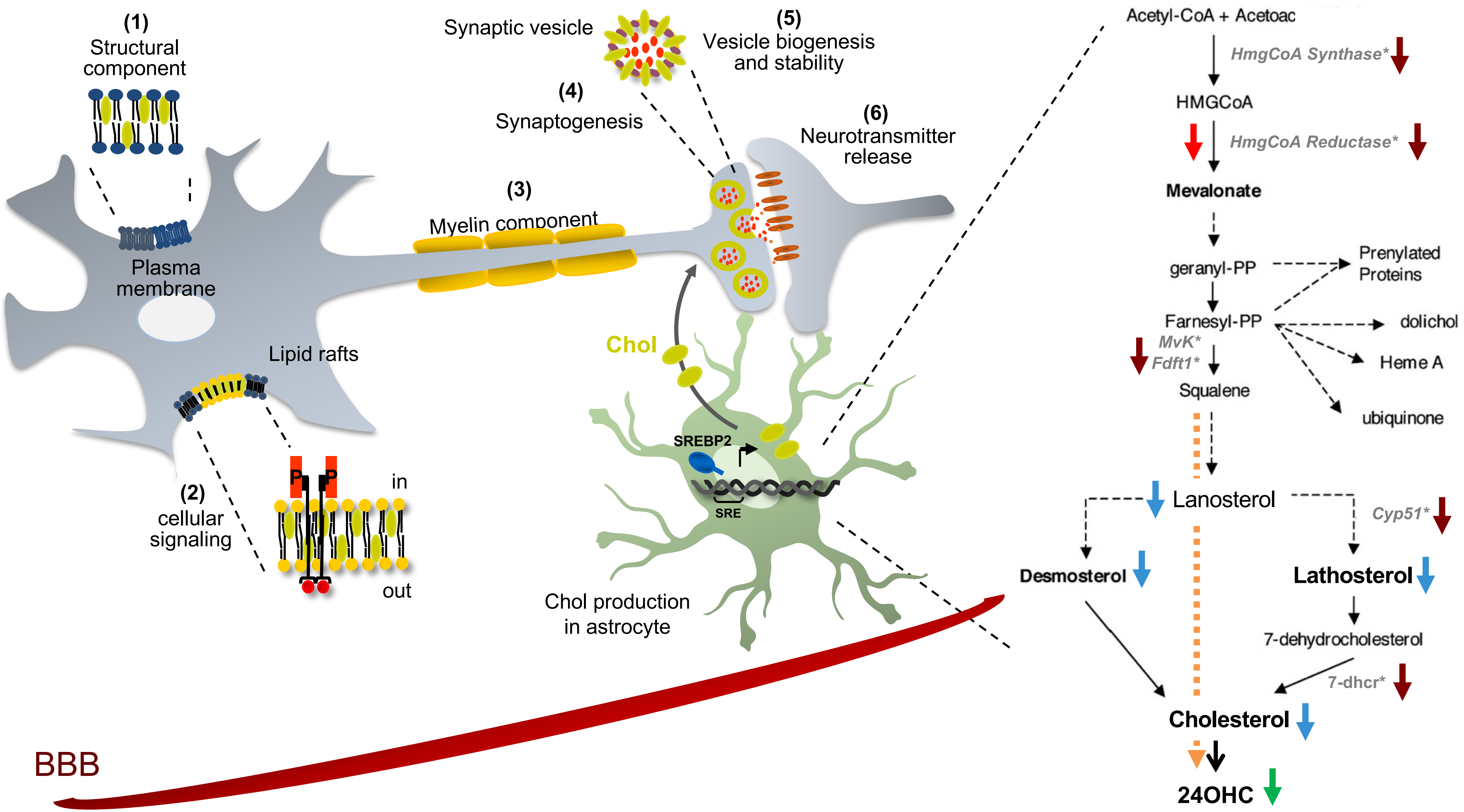

mRNA levels of chol. genes

Sipione et al., 2002; Valenza et al., 2005; Bobrowska et al., 2012; Lee et al., 2014; Al-Dalahmah et al., 2020; Shankaran et al., 2017

HMGCoARed Activity

Valenza et al., 2007a; Valenza et al., 2007b

Chol precursors by ID-MS

Chol content by ID-MS

Valenza et al., 2007a; Valenza et al., 2007b; Valenza et al., 2010; Valenza et al., 2015; Shankaran et al., 2017; Birolini et al., 2020; Birolini et al., 2021

Chol synthesis rate *in vivo*

Shankaran et al., 2017

24S-OHC by ID-MS

24S-OHC synthesis *in vivo*

Valenza et al., 2007; Valenza et al., 2010; Valenza et al., 2015; Boussicalt et al., 2016; Shankaran et al., 2017; Karter et al., 2019; Birolini et al., 2020; Birolini et al., 2021

* SREBP2-dependent genes

Brain cholesterol is essential for normal brain function (Pfrieger, 2003; Orth, 2012). Peripheral cholesterol can not reach the brain due to the presence of the blood brain barrier, thus in the adult brain cholesterol is produced locally by astrocytes (Mauch et al., 2001). Brain cholesterol biosynthesis is early reduced in HD animal models, before the onset of motor defects (Valenza et al., 2005; Valenza et al., 2007; 2010; Shankaran et al., 2017). The underlying molecular mechanism is a a diminished nuclear translocation of the transcription factor sterol regulatory element binding protein 2 (SREBP2) and, consequently, reduced activation of SREBP-controlled genes in the cholesterol biosynthesis pathway (Valenza et al., 2005; 2015; Di Pardo et al., 2020).

Spread and tropism of AAV2/5 vectors in the striatum

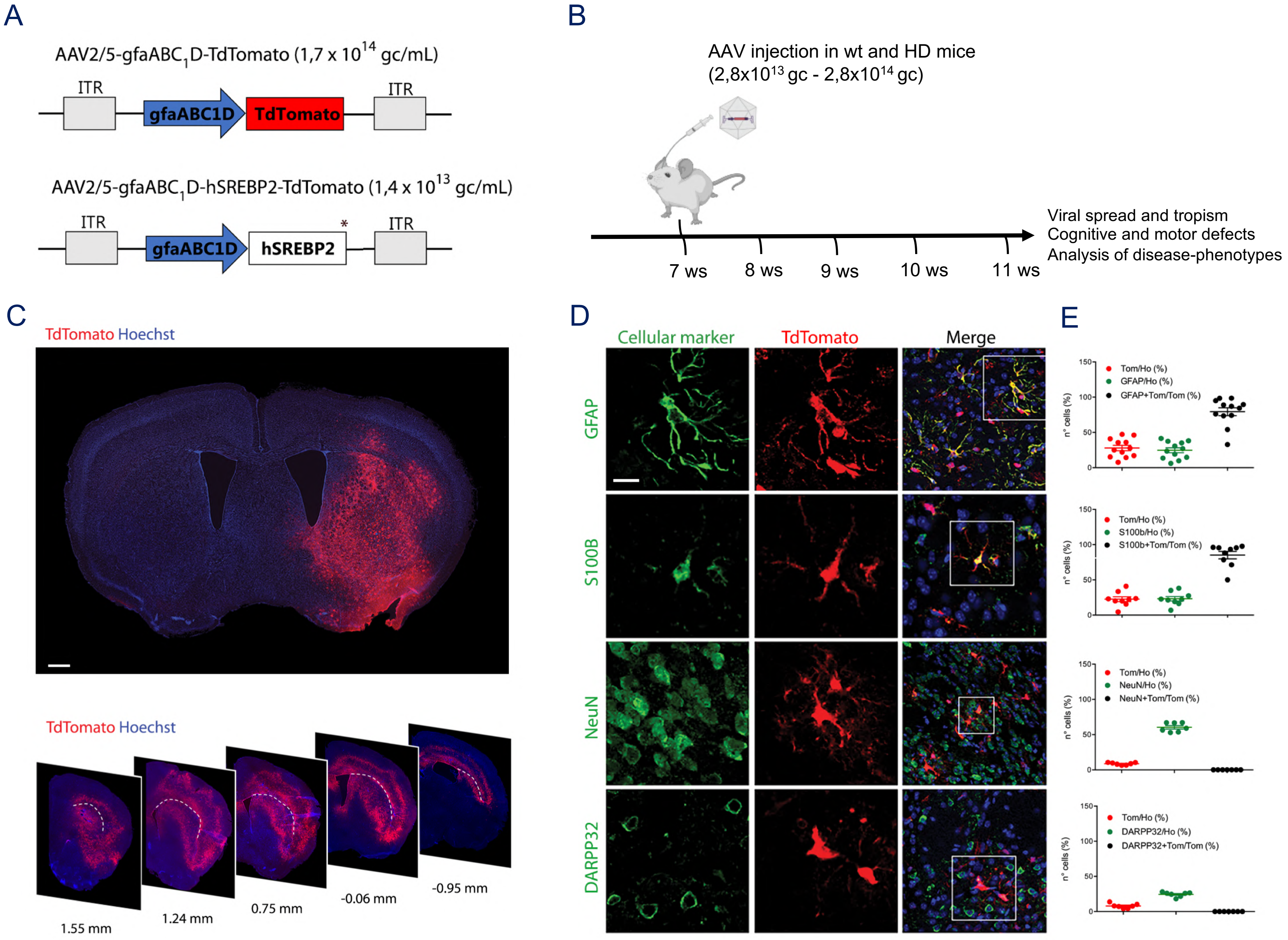

A-B. Scheme of the AAV2/5 vectors and the experimental paradigm used in the study. Wt and R6/2 mice at 7 weeks of age were infected in the right striatum with AAV2/5 vectors and sacrificed 4 weeks later.

C. Representative immunofluorescence large images showing diffusion of tdTomato (red) in coronal brain slices of wt mice infected with AAV2/5-gfaABC1D-tdTomato.

D. Representative immunofluorescence images showing tdTomato labelled cells (red), GFAP and S100b labeled astrocytes (green) and NeuN and DARPP32 labelled neurons (green) in coronal brain slices of mice infected with AAV2/5-gfaABC1D-TdTomato.

E. Relative quantification of the number of cells double positive for tdTomato and for the specific cellular marker, normalized on the number of the nuclei in the field of view (expressed as %)

Birolini et al., Brain 2021

hSREBP2 expression in R6/2 mice following striatal AAV infection

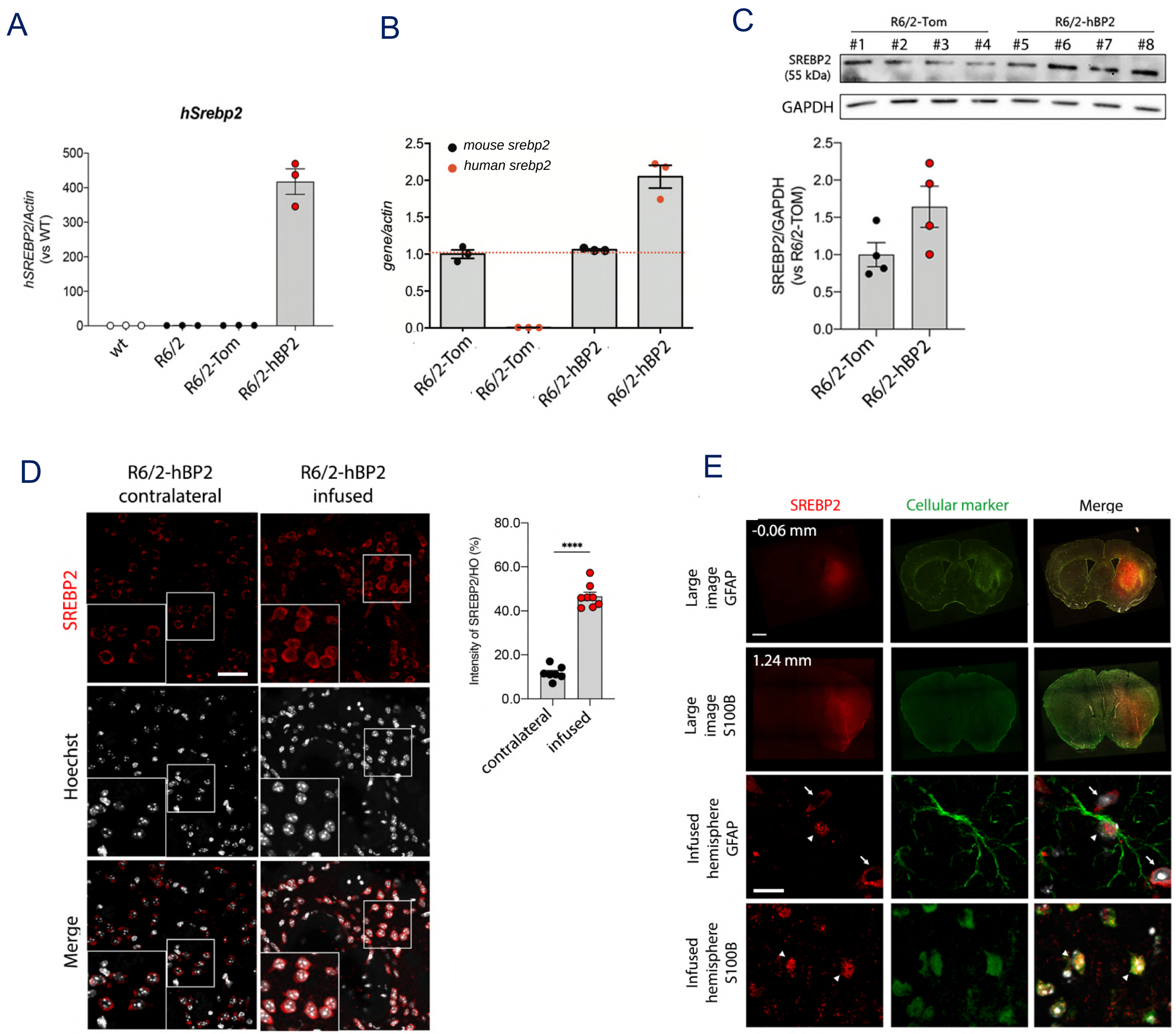

A-B. mRNA levels of *hSrebp2* in the hemibrains from wt, R6/2, R6/2-Tom, and R6/2-hBP2 mice normalized on wt mice and the fold-increased compared to ndogenous mouse *srebp2* (n = 3 mice/group).

C. Level of SREBP2 protein (both endogenous and exogenous) and relative densitometric quantification in protein lysates from the infused hemibrains of R6/2-Tom or R6/2-hBP2 (n = 4 mice/group). GAPDH was used as loading control and for normalization.

D. Representative immunofluorescence image of SREBP2 labelled cells and relative quantification in the infused and contralateral striatum of R6/2-hBP2 mice (n = 4 mice). Graph (I) represents the intensity of SREBP2 normalized on nuclei (%).

E. Representative immunofluorescence large image and high-magnification image of the infused striatum with SREBP2 (red) and GFAP or S100B labelled cells (green) in coronal brain slices of R6/2-hBP2 mice. Nuclear (triangles) and perinuclear (arrows) localization of SREBP2 was indicated. Hoechst was used to counterstain nuclei. Scale bar: 20 µm (D), 2000 µm (E, large image), and 10 µm (E, crop).

*Data are shown as scatterplot graphs with means ± SEM. Statistics: unpaired Student's t test (****p < 0.0001).*

Birolini et al., Brain 2021

hSREBP2 delivery enhances cholesterol biosynthesis in HD mice

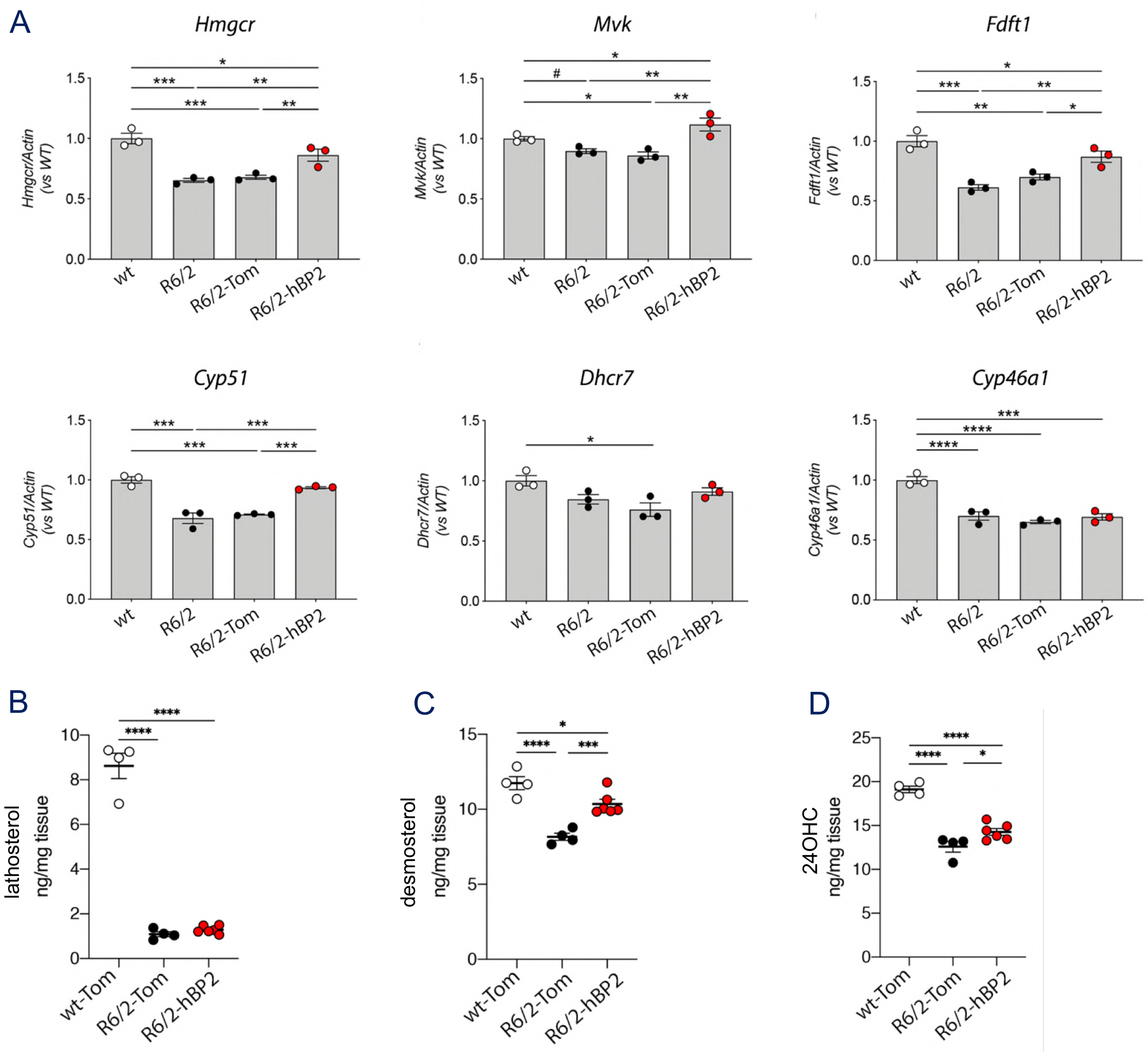

A. mRNA levels of Hmgcr, Mvk, Fdft1, Cyp51, Dhcr7, and Cyp46a1 in the hemibrain from wt, R6/2, R6/2-Tom mice, and R6/2-hBP2 mice (n = 3 mice/group).

SREBP2-dependent genes of cholesterol biosynthesis: Hmgcr: hydroxymethylglutaryl-coenzyme A reductase; Mvk: mevalonate kinase; Fdft1: farnesyl-diphosphate farnesyl transferase 1; Cyp51: cytochrome p450 lanosterol 14-alpha-demethylase; Dhcr7: 7 dehydroxycholesterol reductase

Gene involved in brain cholesterol catabolism:
Cyp46a1: cholesterol 24-hydroxylase.

B-D. Cholesterol precursors (lathosterol, desmosterol) and 24OHC levels in the infused striata of wt-Tom, R6/2-Tom, and R6/2-hBP2 mice (n = 4–6 mice/group).

Data are shown as scatterplot graphs with means ± SEM. Each dot corresponds to the value obtained from each animal.

*Statistics: one-way ANOVA with Newman–Keuls post-hoc test (*p < 0.05; **p < 0.01; ***p < 0.001; **** p < 0.0001) or unpaired Student's t-test (#p < 0.05).*

Birolini et al., Brain 2021

hSREBP2 delivery restores synaptic communication in HD mice

A Spontaneous synaptic events

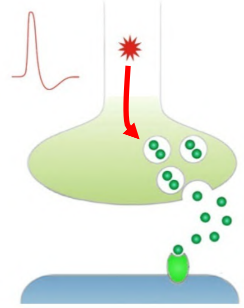

B Glutamatergic activity

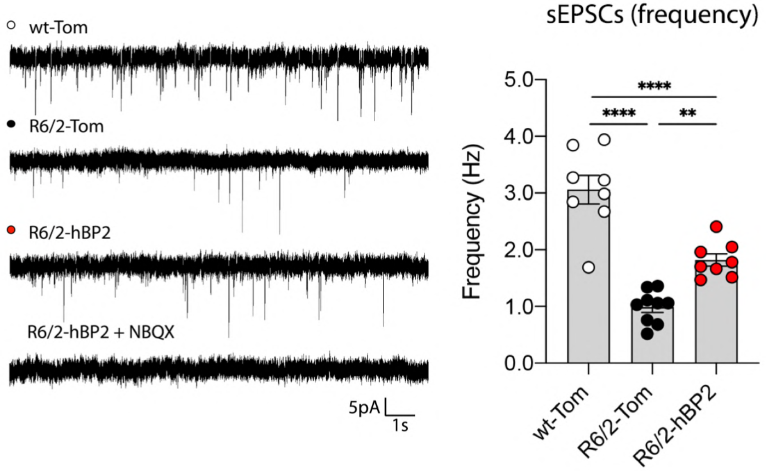

C GABAergic activity

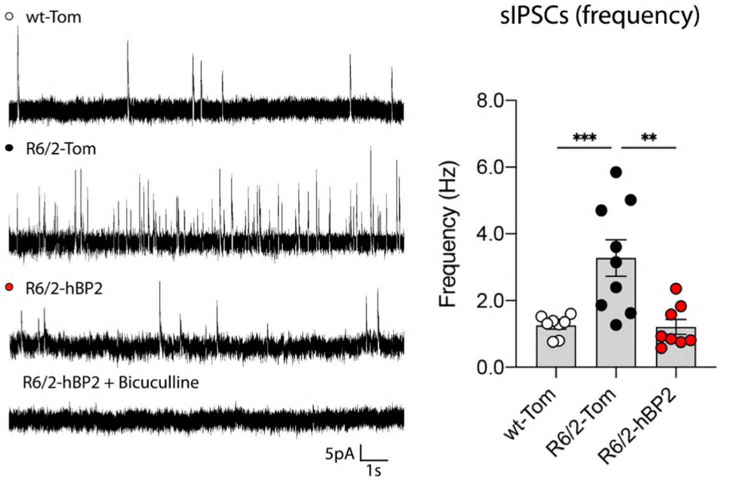

D Miniature synaptic events

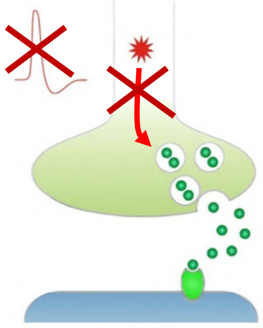

E

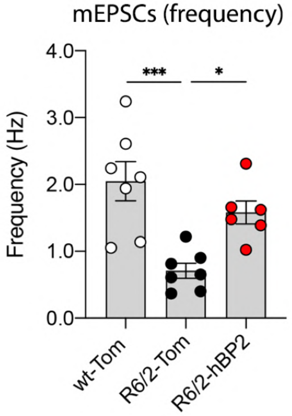

F

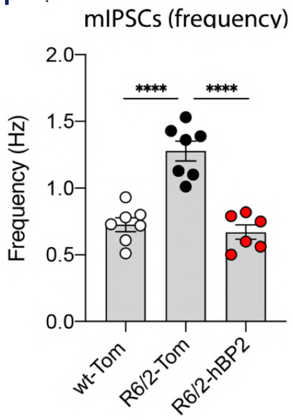

A. Schematic representation of the spontaneous synaptic events recorded in striatal MSNs of wt and R6/2 mice following 4 weeks of AAV2/5 injections.

B. Representative traces of spontaneous EPSCs (sEPSCs) recorded from MSNs at a holding potential of -70 mV from striatal MSNs from wt-Tom, R6/2-Tom, and R6/2-hBP2 mice. Average frequency of sEPSCs recorded from MSNs of wt-Tom, R6/2-Tom, and R6/2-hBP2 mice.

C. Representative traces of spontaneous IPSCs (sIPSCs) recorded from MSNs at a holding potential of 0 mV from striatal MSNs from wt-Tom, R6/2-Tom, and R6/2-hBP2 mice. Average frequency of sIPSCs recorded from MSNs of wt-Tom, R6/2-Tom, and R6/2-hBP2 mice.

D. Schematic representation of the miniature synaptic events recorded in the same striatal MSNs. **E-F.** Average frequency of miniature EPSCs (mEPSCs) and of miniature IPSCs (mIPSCs) recorded from wt-Tom, R6/2-Tom, and R6/2-hBP2 mice MSNs, in presence of the Na+ channel blocker tetrodotoxin (TTX, 1μM).

*Statistics: one-way ANOVA with Newman–Keuls post-hoc test (*p < 0.05; **p < 0.01; ***p < 0.001; ****p < 0.0001).*

Birolini et al., Brain 2021

hSREBP2 delivery reduces muHTT aggregates in HD mice

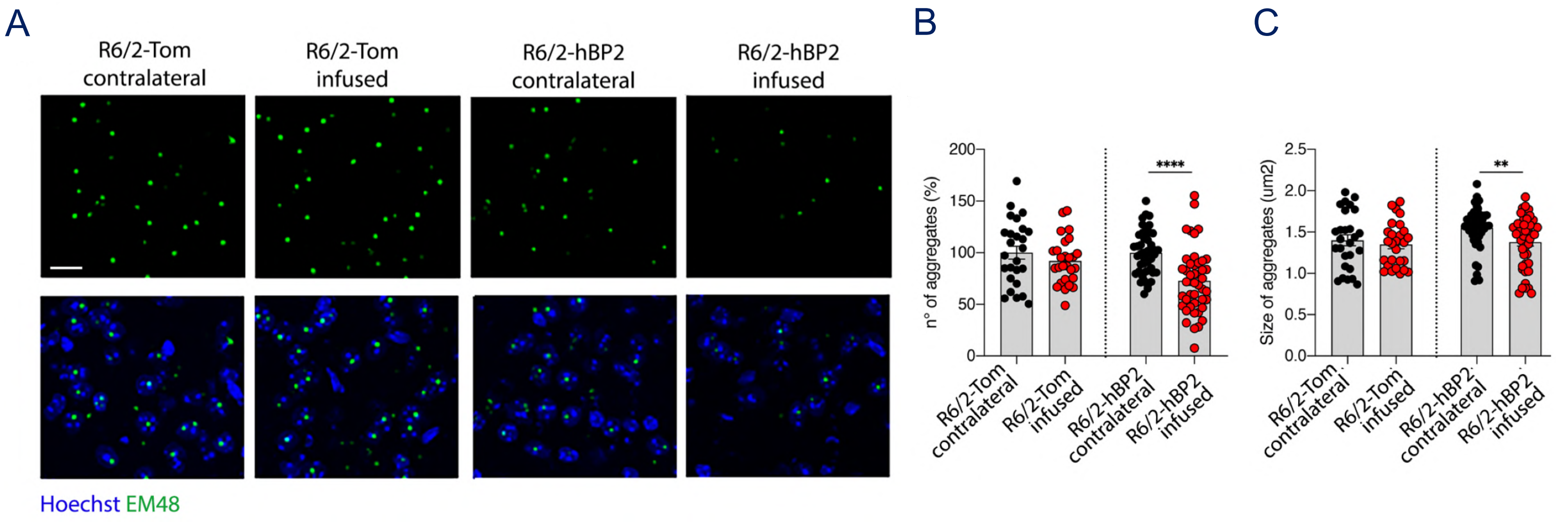

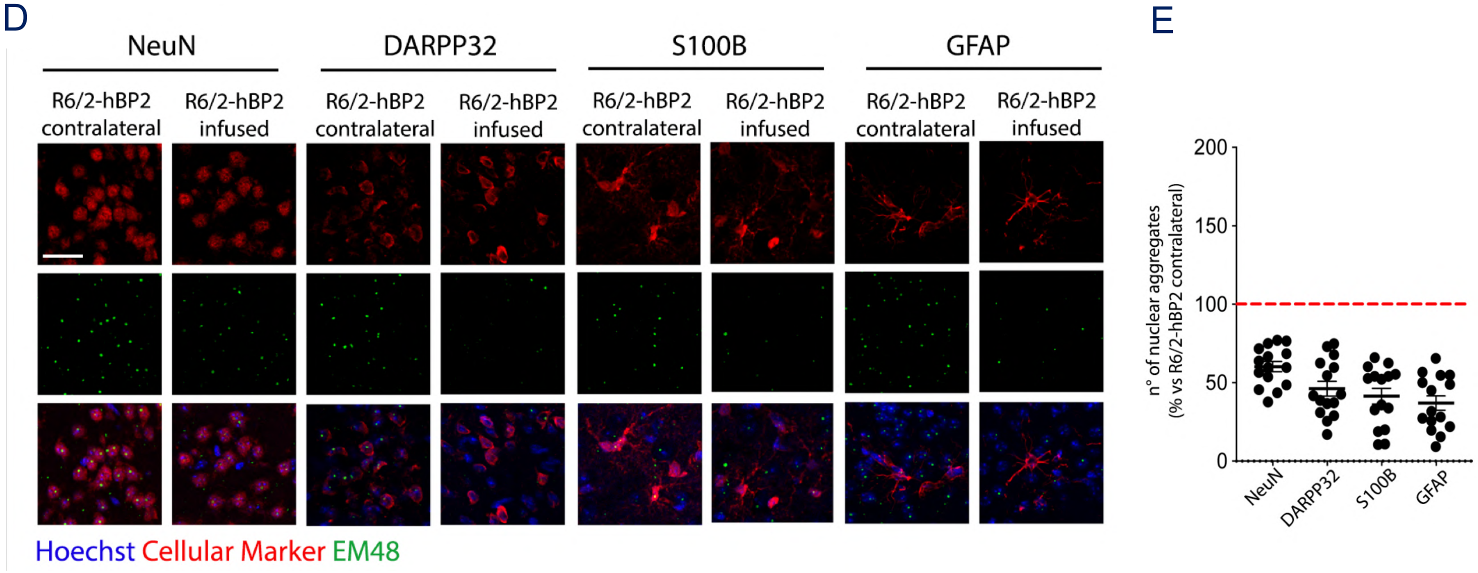

A-C. Representative immunofluorescence images of muHTT aggregates positive for EM48 antibody (green) (A) and relative quantification of number (B) and size (C) in infused and contralateral striata of R6/2-Tom mice or R6/2-hBP2 mice (n = 3–5/group). The number of muHTT aggregates (B) in the infused hemisphere was normalized on the contralateral one.

D-E. Representative immunofluorescence images showing muHTT aggregates (EM48 antibody, green) in NeuN and DARPP32 labelled neurons (red) or in S100B and GFAP labelled astrocytes (red) (D) in infused and contralateral striata of R6/2-hBP2 mice (n = 3/group), and relative quantification of the number of muHTT aggregates in the infused hemisphere normalized on the contralateral one (E).

Data are shown as scatterplot graphs with means ± SEM. Each dot corresponds to an image from 3-5 mice/group. Hoechst (blue) (A and D) was used to counterstain nuclei. Scale bars: 10 µm (A), 25 µm (D).

Statistics: one-way ANOVA with Newman–Keuls post-hoc test $**p < 0.01$; $****p < 0.0001$).

Birolini et al., Brain 2021

hSREBP2 delivery increases Drd2-expressing MSNs in HD mice

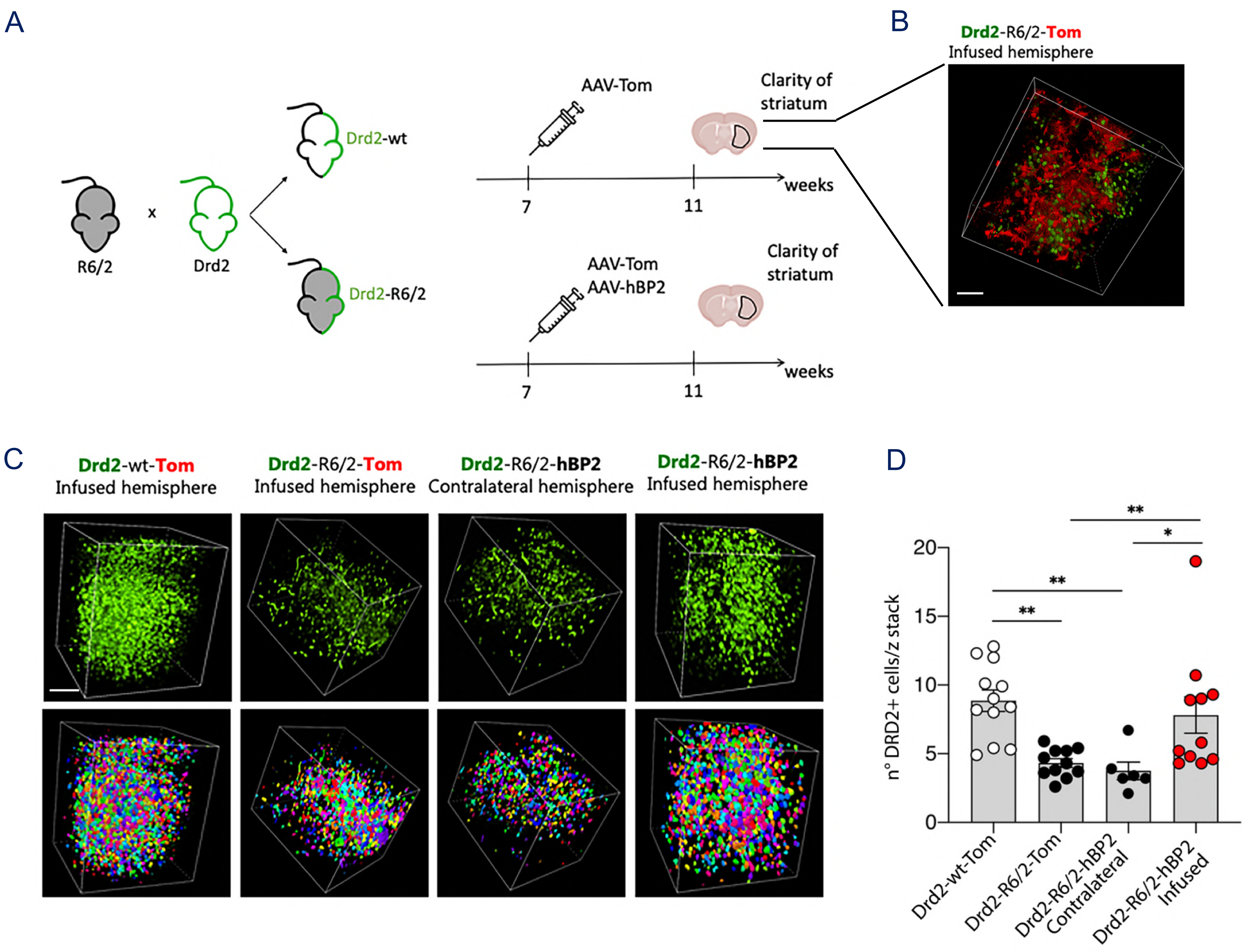

A. Experimental paradigm used in the CLARITY experiment. R6/2 mice were crossed with mice having Drd2-expressing MSNs tagged with GFP to obtain an HD line with GFP-MSNs neurons from the indirect pathway. Mice were sacrificed 4 weeks later and two 1 mm-thick brain coronal slices (comprehending the striatum) were prepared from each animal. From each slice, the portion including the infused and the contralateral striatum was isolated and clarified using the X-CLARITY technology (n = 4-5 mice/group).

B. Representative two-photon image of the endogenous signals of GFP (green) and TdTomato (red) of 1-mm thick brain coronal slices from Drd2-wt-Tom (infused hemisphere). Scale bars: 100 µm.

C-D. Representative two-photon images (up) of the endogenous signal of GFP (green) of 1-mm thick brain coronal slices from Drd2-wt-Tom (infused hemisphere), Drd2-R6/2-Tom (infused hemisphere), and Drd2-R6/2-hBP2 (contralateral and infused hemisphere) with relative 3D reconstruction (down) and quantification of the number of neurons normalized on the z-stack acquired. Scale bars: 200 µm (C).

*Statistics: one-way ANOVA with Newman–Keuls post-hoc test (*p < 0.05; **p < 0.01).*

Birolini et al., Brain 2021

hSREBP2 delivery restores motor and cognitive defects in HD mice

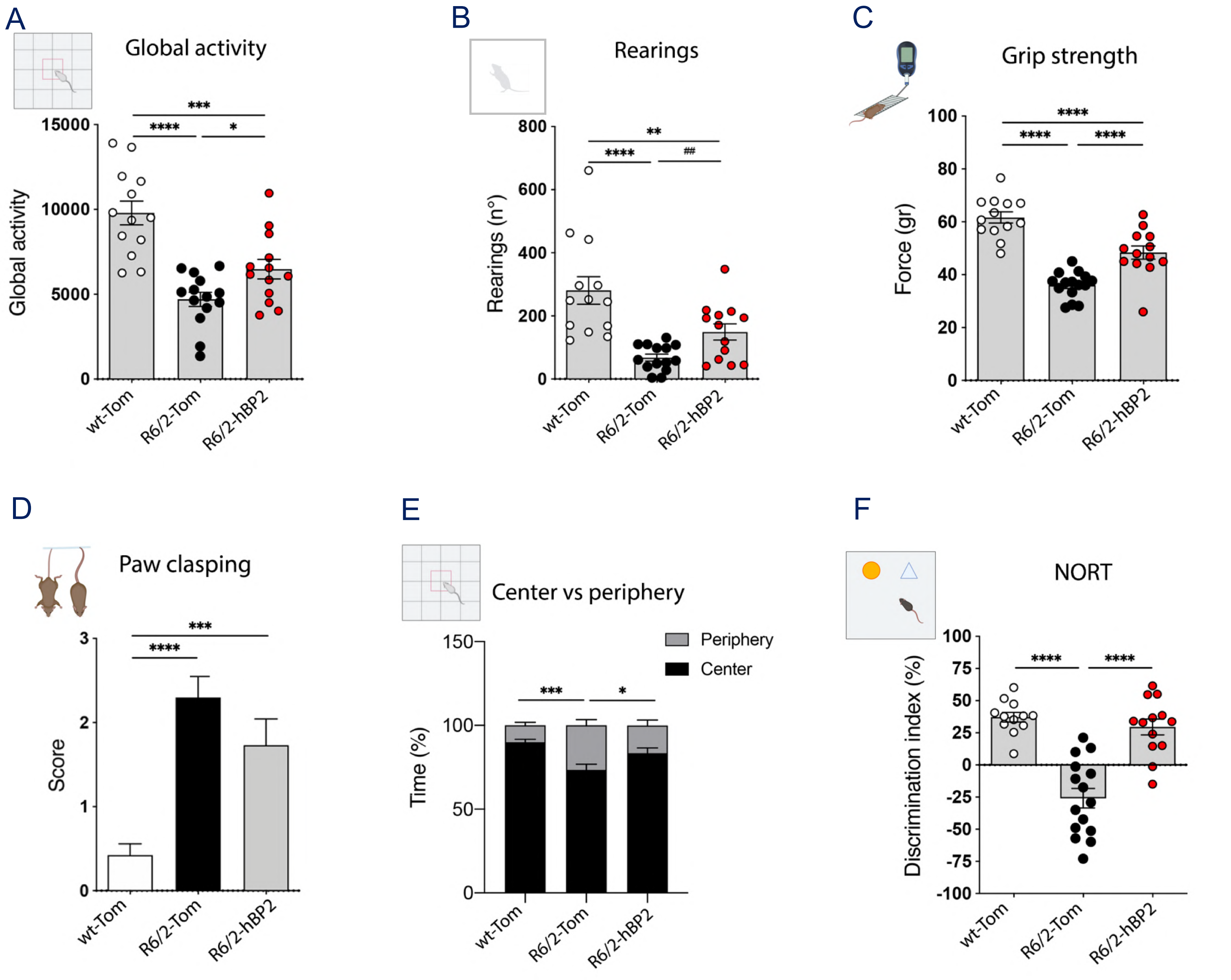

A-B. Global activity and number of rearings in an open-field test in wt-Tom (n = 13), R6/2-Tom (n = 14), and R6/2-hBP2 (n = 13).

C. Grip strength (grams) in wt-Tom (n = 13), R6/2-Tom (n = 15), and R6/2-hBP2 (n = 13).

D. Paw clasping in wt-Tom (n = 13), R6/2-Tom (n = 15), and R6/2-hBP2 (n = 13).

E. Quantification (E) of the time spent (%) in the center and in the periphery of the arena in the open-filed test in wt-Tom (n = 13), R6/2-Tom (n = 14), and R6/2-hBP2 (n = 13).

F. Discrimination index (DI %) in the novel object recognition test of wt-Tom (n = 12), R6/2-Tom (n = 15), and R6/2-hBP2 (n = 13). DI above zero indicates a preference for the novel object; DI below zero indicates a preference for the familiar object.

Data (A-C and F) are shown as scatterplot graphs with means ± SEM and each dot corresponds to the value obtained from each animal. Data (D and E) are shown as histograms with means ± SEM.

*Statistics: one-way ANOVA with Newman–Keuls post-hoc test (*p < 0.05; **p < 0.01; ***p < 0.001; ****p < 0.0001) or unpaired Student's t-test (##p < 0.01).*

Birolini et al., Brain 2021

Conclusions

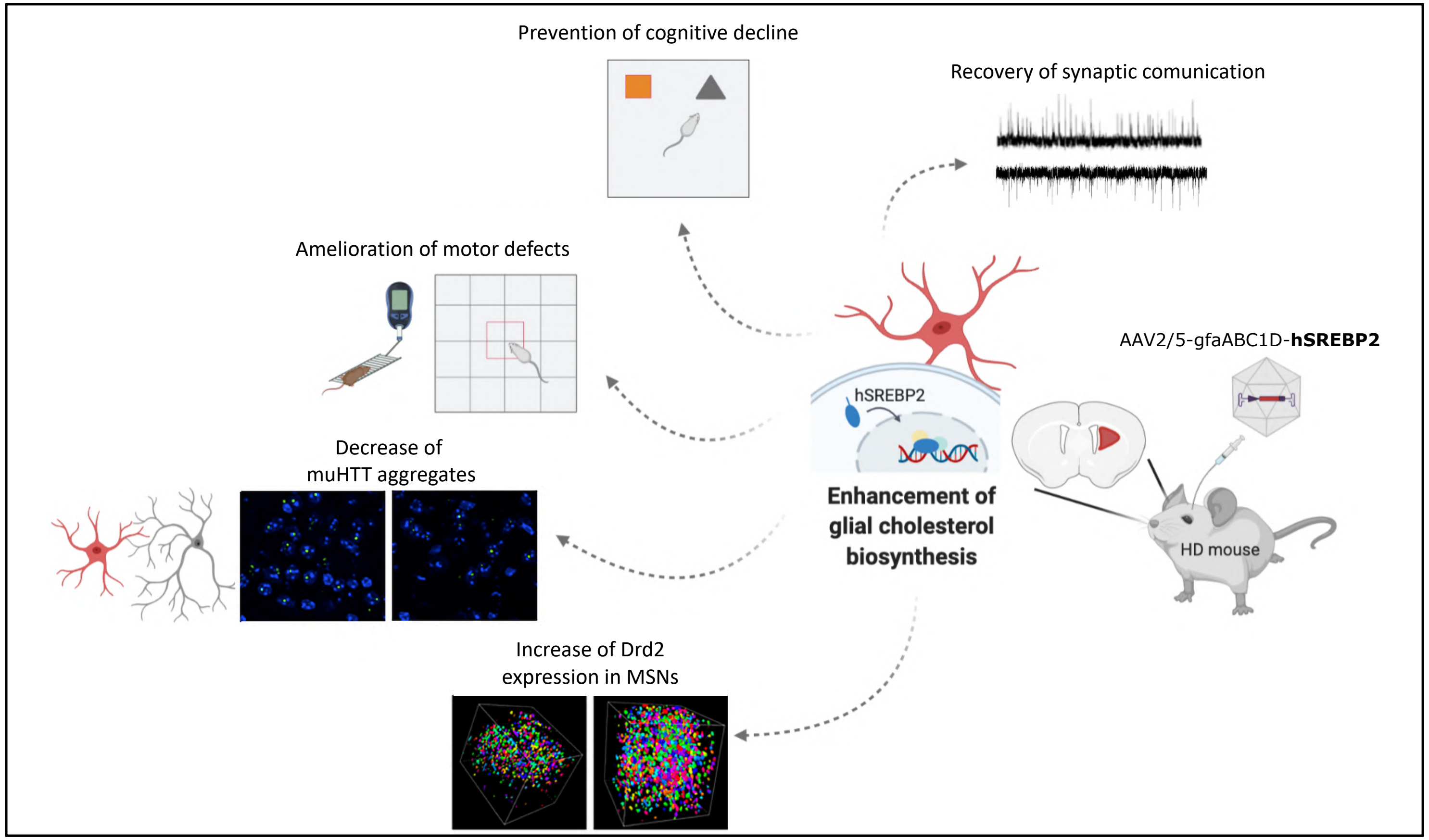

- Cholesterol biosynthesis in astrocytes is relevant for brain function and behavior in HD
- AAV-based delivery of SREBP2 to astrocytes counteracts key features of HD
- These findings may provide the foundation for new therapeutic strategies